The changing thermal state of permafrost

Sharon L. Smith[1] ✉, *H. Brendan O'Neill*[1], *Ketil Isaksen*[2], *Jeannette Noetzli*[3] *and Vladimir E. Romanovsky*[4]

Abstract | Permafrost temperatures have increased in polar and high-elevation regions, affecting the climate system and the integrity of natural and built environments. In this Review, we outline changes in the thermal state of permafrost, focusing on permafrost temperatures and active-layer thickness. Increases in permafrost temperature vary spatially owing to interactions between climate, vegetation, snow cover, organic-layer thickness and ground ice content. In warmer permafrost (temperatures close to 0 °C), rates of warming are typically less than 0.3 °C per decade, as observed in sub-Arctic regions. In colder permafrost (temperatures less than −2 °C), by contrast, warming of up to about 1 °C per decade is apparent, as in the high-latitude Arctic. Increased active-layer thicknesses have also been observed since the 1990s in some regions, including a change of 0.4 m in the Russian Arctic. Simulations unanimously indicate that warming and thawing of permafrost will continue in response to climate change and potentially accelerate, but there is substantial variation in the magnitude and timing of predicted changes between different models and scenarios. A greater understanding of longer-term interactions between permafrost, climate, vegetation and snow cover, as well as improved model representation of subsurface conditions including ground ice, will further reduce uncertainty regarding the thermal state of permafrost and its future response.

Permafrost is a key component of the cryosphere, defined as ground that remains at or below 0 °C for at least two consecutive years. Near the surface, ground temperatures fluctuate in response to high-frequency variations in air temperature and snow cover. At greater depths, however, ground temperature changes are attenuated and delayed (BOX 1). Seasonal variations become negligible at the depth of zero annual amplitude (DZAA)[1], making the temperature at this depth a suitable indicator of long-term change in permafrost thermal state. Active-layer thickness (ALT) — the layer above permafrost that freezes and thaws annually — is a further important characteristic of permafrost environments. Together, the temperature at the DZAA and ALT are variables that are monitored to track long-term changes in the thermal state of permafrost, which is vital given the pronounced atmospheric warming observed in polar and high mountain areas[2,3]. Indeed, the thermal state of permafrost is a key indicator of anthropogenic warming, with long-term changes increasingly apparent[4–9]. Since the 1980s, for example, permafrost near the DZAA has warmed by 1 to 3 °C in some Arctic and mountain regions. There is further widespread evidence and documentation of permafrost thawing[5–7].

Given that permafrost is a key component of polar and high-elevation landscapes, any changes can have substantial consequences for natural and human systems[6,7]. For instance, warming and subsequent thawing of permafrost can affect landscape stability, causing subsidence of the ground surface, slope instability, rock glacier acceleration and changes to hydrological processes[7,10–13]. This reduction in ground stability affects the integrity of infrastructure[6,7,14,15]. High-latitude and some high-elevation permafrost areas (for example, that underlying the Tibetan Plateau) also store large amounts of carbon that become mobilized and released as greenhouse gases upon thawing, influencing feedbacks with the climate system[6,16,17]. Knowledge of the current and projected future thermal state of permafrost is, therefore, integral to our understanding, enabling us to minimize impacts on the natural environment and informing the design of resilient infrastructure.

In this Review, we synthesize knowledge of the thermal state of permafrost in a changing climate. We begin by summarizing evidence of change, focusing on permafrost temperature and ALT. We next outline the key drivers of observed changes and discuss the limitations and challenges of existing observation systems and techniques. We further outline projections of

[1]*Geological Survey of Canada, Natural Resources Canada, Ottawa, ON, Canada.*

[2]*Norwegian Meteorological Institute, Oslo, Norway.*

[3]*WSL Institute for Snow and Avalanche Research SLF, Davos-Dorf, Switzerland.*

[4]*Geophysical Institute, University of Alaska Fairbanks, Fairbanks, AK, USA.*

✉*e-mail: sharon.smith@nrcan-rncan.gc.ca*

https://doi.org/10.1038/s43017-021-00240-1

Key points

- Widespread and persistent warming of permafrost is observed in polar regions and at high elevations since about 1980, at rates that vary regionally.
- The highest permafrost temperatures in the instrumental record were recorded in 2018–2019 at most sites in Arctic and sub-Arctic regions.
- Trends in permafrost warming are consistent with trends in air temperature. However, local conditions including snow cover and vegetation modulate the response of permafrost under a warming climate.
- Permafrost is projected to continue to warm and thaw in response to climatic warming, but there is uncertainty with respect to the magnitude and timing of these changes.

future permafrost conditions and limitations of different modelling approaches, before providing future research priorities and knowledge gaps.

Observed changes in thermal state

As ground temperatures at depth cannot be observed using satellite or airborne techniques, monitoring changes in the thermal state of permafrost is challenging. However, direct field measurements of ground temperatures at depth and active-layer thickness provide documentation of changing permafrost conditions in many areas, particularly in the Northern Hemisphere.

Observation networks. Temperatures measured in boreholes — typically drilled to depths of 20–30 m, below the DZAA, to represent longer-term climatic changes — allow direct, quantitative and comparable observations of permafrost thermal state. Ground temperature monitoring sites typically consist of boreholes instrumented with multi-sensor cables to measure temperature at several depths. The Global Terrestrial Network for Permafrost (GTN-P), an international programme of the Global Climate Observing System, currently includes over 200 boreholes distributed throughout permafrost regions[18,19], including: the Arctic and sub-Arctic regions of North America, Russia and the Nordic countries; mountain and high-elevation regions of Europe and Asia; and Antarctica[4]. However, large spatial gaps exist in the monitoring network owing to the costly and challenging logistics of borehole installation in remote circumpolar regions and mountain areas with steep and complex topography. Site selection has therefore historically favoured locations near communities, critical infrastructure and areas of specific research interests, but existing sites nevertheless encompass a broad range of geologic and ecoclimatic conditions.

Although some sites in polar areas have been in operation for more than 40 years, most were established during or since the International Polar Year (IPY; 2007–2009). Other regional efforts have focused on nonpolar regions, such as the Permafrost and Climate in Europe project[20], which established monitoring sites to extend and support ongoing monitoring of European mountain permafrost[8,21], and other programmes in Antarctica[22] and high-elevation areas of Asia[23].

To monitor ALT, frost probing in late summer or early autumn, near the time of maximum thaw, is the most frequently used method. These ALT measurements have been collected at many sites since the 1990s, particularly as part of the Circumpolar Active Layer Monitoring (CALM) network in the Arctic, Antarctic and high-elevation and mountain permafrost regions[24], and of other regional programmes[25,26]. Other methods to determine ALT include the use of thaw tubes or interpolation of the 0 °C isotherm from shallow ground temperature measurements[27], the latter of which is the only practical method in areas dominated by debris and bedrock slopes[28].

Continuous operation of these monitoring sites has allowed annual updates to ground temperature time series and ALT records, informing key assessments[4–7,29–32]. Several early regional and local-scale investigations documented changes in permafrost temperatures in North America[33–36], Siberia[37], Europe and Scandinavia[21,38,39], and the Tibetan Plateau[40]. However, it was the IPY that spurred the first comprehensive synthesis of the permafrost thermal state at a circum-Arctic scale[19]. A major achievement of this effort was the establishment of a temperature baseline from which to assess future change. Regional syntheses placed the conditions during the IPY in the context of the longer record (where available), providing documentation of changes over time[41–43]. These regional syntheses presented evidence of increasing permafrost temperatures, in some cases since the 1970s up to the IPY, for several Arctic areas[19].

Permafrost temperature changes. Widespread and persistent warming is observed in most contemporary global assessments of permafrost temperatures measured at or near the DZAA[4,29,30] (FIG. 1). However, there is considerable regional variability in the magnitude of this warming owing to differences in the proximity of permafrost temperatures to 0 °C, substrate properties (including ground ice), and snow and vegetation conditions. In particular, temperature changes differ substantially between continuous and discontinuous permafrost domains.

The highest permafrost temperatures in the instrumental record, which spans more than three decades at some sites, were recorded in 2018–2019 at most sites in Arctic and sub-Arctic regions (FIG. 2a,b). Maximum temperature increases are typically evident in the cold Arctic ground of the continuous permafrost region (FIGS 1,2a). For instance, warming rates of 0.4–0.8 °C per decade have occurred since the 1980s in northern Alaska and in the northern Mackenzie Valley[30,44], and up to 0.7 °C per decade in northern Quebec and on Baffin Island[5,31,45]. At the high-latitude Arctic station of Alert on Ellesmere Island, similar increases of 0.4–0.6 °C per decade have been apparent since the 1980s. Here, twenty-first-century warming rates have been greater (0.6–1.1 °C per decade) than for the entire record (which started in 1978), as is also the case with temperature trends further south in the Baffin region[30]. Permafrost temperature increases on the Arctic Svalbard archipelago and Russia are also similar, typically reaching 0.8 °C per decade[8,30] and 0.5 °C per decade[30,46,47], respectively. However, warming rates of 0.9 °C per decade have been recorded in some Siberian boreholes since 2008 (REF.[4]).

In the warmer ground of the discontinuous permafrost zone, by contrast, temperature increases are typically

Box 1 | **Features of the ground thermal regime in permafrost**

The thermal characteristics of permafrost include various features and metrics (see the figure, left panel). Near-surface ground temperatures generally respond to the annual cycle of air temperature. Temperature variation decreases with depth, becoming negligible at the depth of zero annual amplitude (DZAA), which for practical purposes is where annual fluctuations are <0.1 °C. The DZAA depends on the thermal properties of the ground, influenced by material type, moisture and ice content. For example, the DZAA is greater in bedrock with a high quartz content (>20 m) compared to fine-grained silt or organic material (<10–15 m). Below the DZAA, temperature increases with depth owing to the geothermal gradient. In flat terrain, variations in the geothermal gradient with depth are indicators of climatic fluctuations[169].

The permafrost layer occurs where temperatures remain ≤0 °C. The active layer is the layer of ground above permafrost that thaws and freezes annually. Differences in the thermal conductivity of frozen and thawed materials in this layer can result in mean annual temperature being higher at the ground surface compared to the top of the permafrost layer. This effect is referred to as the thermal offset[98,100], the magnitude of which is greater in material with higher moisture contents, although the effects of non-conductive heat transport are also a factor[170]. The thermal offset means that permafrost can exist even in areas where annual mean ground surface temperatures are above 0 °C. The surface offset is defined as the difference between the annual mean ground surface temperature and the annual mean air temperature, and reflects the buffering effect of snow and vegetation cover[98,171], and the influence of solar radiation on the surface energy balance[51,170].

As air and ground surface temperatures rise, increases in ground temperature will occur in the near-surface and gradually propagate to greater depths. The ground acts as a filter with higher-frequency variability in temperature reduced at greater depths, such that only longer-term changes in temperature are preserved at depths beyond the DZAA. Temperature changes at depth lag behind those at the surface, with the lag increasing with depth (see the figure, right panel). Therefore, deeper ground temperatures can provide a record of temperature changes over past decades or centuries or longer[149,172], and can be used to reconstruct the past history of surface temperatures[75,173,174].

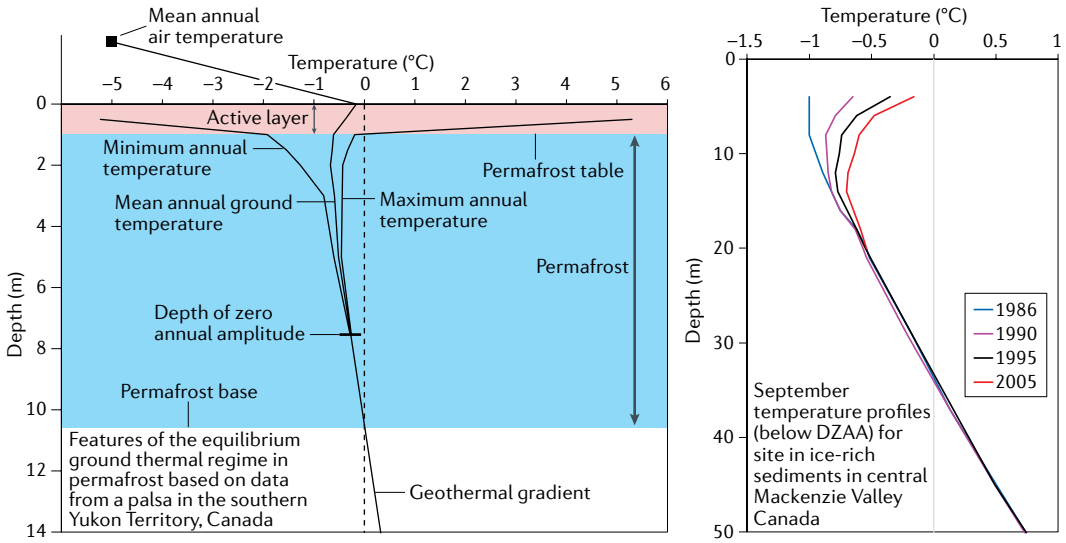

smaller (FIGS 1,2b). Indeed, since the 1980s, warming at or near the DZAA has ranged from <0.1–0.3 °C per decade in discontinuous permafrost of Alaska and the Mackenzie Valley, with less change observed where permafrost temperatures are near 0 °C (REF.[30]). Similar warming rates have occurred since the late 1970s and early 1980s in southern Yukon[31]. As in North America, smaller temperature increases have been recorded in northern Scandinavia and southern Norway where ground temperatures are higher[8,29] (typically 0.1–0.5 °C per decade), as well as in the warmer regions of the Russian European north and northwest Siberia[30,46,47] (0.2 °C per decade).

In Antarctica, permafrost monitoring sites have been established more recently than those in the Northern Hemisphere, and there is a limited number of boreholes that extend beyond the DZAA. While there is some indication of temperature increases at shallower depths since about 2010 (REF.[4]), longer-term trends are not as evident at greater depths[48].

The thermal state of permafrost has also been monitored in high-elevation areas of the Northern Hemisphere such as the European Alps and the Tibetan Plateau. In the European Alps, as with the Arctic, warming rates are generally higher for colder permafrost[8,26,29], with temperature increases comparable to those of the Arctic for ice-poor shaded bedrock sites at high elevations (FIGS 1,2c). For example, the longest record, spanning >30 years, is observed in an ice-rich rock glacier in the Swiss Alps, where temperatures have increased by about 0.2 °C per decade, as measured at 20 m depth. On the Tibetan Plateau, where permafrost temperatures are typically higher than −3.0 °C, warming of up to 0.25 °C per decade has been observed since 2000 at depths of 15 m (REF.[32]). Although permafrost also exists in other mountain ranges, including the Himalayas[49,50], North America[51,52], the Andes[53–55] and New Zealand[56], records are not sufficiently long or from great enough depths to allow trends comparable to other areas to be determined.

Fig. 1 | **Trends in permafrost temperatures from monitoring sites.** Permafrost zones[167] (blue shading) and trends in permafrost temperature measured at or near the depth of zero annual amplitude (circles). The circle sizes are proportional to the magnitude of temperature trends for the entire instrumental record (orange) and for 2000–2019 (red). The range for the period is shown by the smaller and larger circles of the same colour. Coloured rectangles indicate that reported trends are from multiple sites in the region. See Supplementary Table 1 for further information on the data sources. Permafrost is warming in all regions, with greater rates of warming occurring in the Arctic.

Active-layer thickness changes. Variations in shallow ground temperatures lead to changes in ALT. In contrast to changes in deeper permafrost temperatures, however, ALT variations are primarily controlled by seasonal air temperatures and snow cover, and thus exhibit inter-annual variation that can obscure longer-term trends. Despite these difficulties, ALT trends can be derived from records of sufficient length.

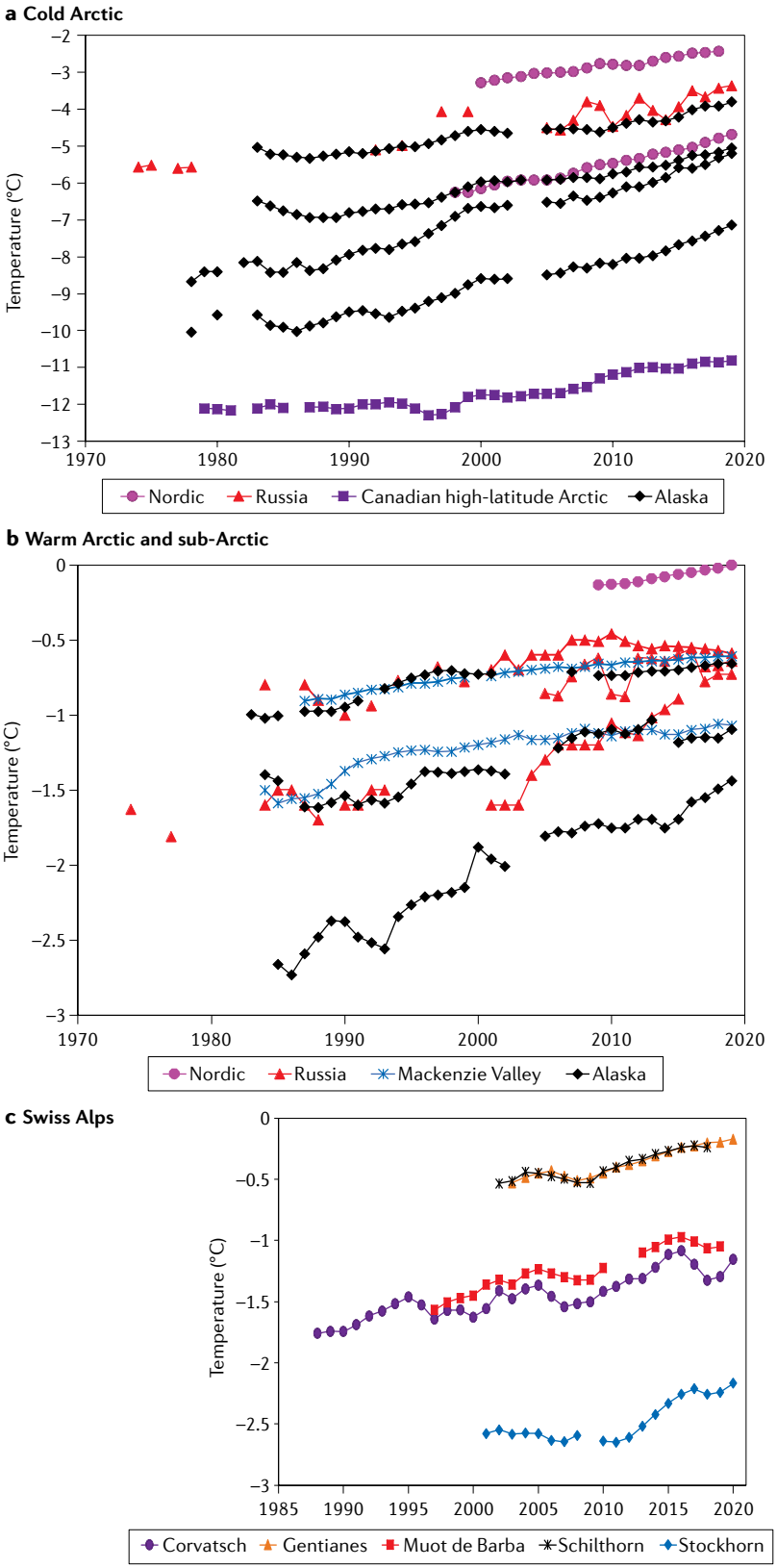

Fig. 2 | **Permafrost temperature time series.** Permafrost temperatures at selected long-term monitoring sites in regions of cold Arctic permafrost[30] (panel **a**), warm Arctic and sub-Arctic permafrost[30] (panel **b**) and the Swiss Alps[26] (panel **c**). Temperatures are measured at or near the depth of zero annual amplitude. Sites were chosen to represent the range in permafrost temperature in different regions. Note the contrasting *y* axes. See Supplementary Table 2 for site information. Permafrost temperatures have been increasing over time in all regions.

ALTs have increased in some regions of the Arctic since the 1990s, although with marked variability (FIG. 3; TABLE 1). ALT trends are most evident in the Russian Arctic[57] (FIG. 3a,b; TABLE 1). Indeed, some of the greatest increases since the late 1990s have been recorded in the Russian European north and western Siberia[30] (FIG. 3a), where average ALT values increased by up to 0.4 m between 1999 and 2019. In North America, some regions have also exhibited substantial changes, but at a lesser magnitude than observed in Russia. In particular, ALT increased by >0.2 m from 1996 to 2019 in the Alaskan interior[30] (FIG. 3c). By contrast, on the Alaskan North Slope (FIG. 3d) and in the Mackenzie Valley (FIG. 3e), ALT decreased following a 1998 peak, and underwent a slight increase since the mid-2000s[25,30]; however, present-day ALTs remain relatively unchanged from those measured before 1998. At sites in southern Norway, northern Sweden, northeast Greenland and central Svalbard, ALT has generally increased since the 1990s at an average rate similar to the Russian Arctic (FIG. 3f; TABLE 1), but with considerable inter-annual variation[8,58].

Decreases in seasonal freezing depths and increases in seasonal thaw depths have also been observed. The ground above permafrost did not completely refreeze in winter 2017–2018 and 2018–2019 at several sites in the Alaskan interior and on Seward Peninsula, indicating formation of a suprapermafrost talik[30], a zone of unfrozen ground above permafrost[59]. Similarly, refreezing above permafrost has not occurred over the past several winters at sites in the Russian European north and in west Siberia[30].

In the ice-free regions of Antarctica, ALT has been monitored at 16 sites since 2006. Here, inter-annual variability is high, with no evidence of longer-term increasing trends[60] (FIG. 3g; TABLE 1). In fact, a decrease in ALT was observed on the western Antarctic Peninsula[61].

Pronounced increases in ALT have been observed in the European Alps since the 1990s (FIG. 3h; TABLE 1). Present-day ALTs are typically >10% above the mean for the entire period[8]. Moreover, ALT has doubled since about 2000 at several sites in the Swiss Alps, increasing by up to several metres[26]. These changes have generally been lower at sites with ice-rich permafrost, such as in rock glaciers, than in bedrock sites. On the Tibetan Plateau, ALT has tended to increase at a rate of about 0.2 m per decade since 1980 (REF.[32]).

Challenges in interpreting trends. Although ground temperatures and ALT have been used to assess changes in permafrost conditions, it is important to be aware of some of the challenges in interpreting the trends from these records. One such challenge is that temperature records from warm permafrost areas can obscure important physical processes active during permafrost degradation. Increases in permafrost temperature have generally been smaller in warmer permafrost close to 0 °C, particularly in ice-rich fine-grained material[7] (FIG. 2b). As permafrost temperatures approach 0 °C, ground ice melts over a range of sub-zero temperatures. Latent heat is required in this phase change, leading to a lower apparent thermal diffusivity and less energy directed at raising ground temperatures[19,43,62–64]. Decreases in resistivity measured by long-term electrical

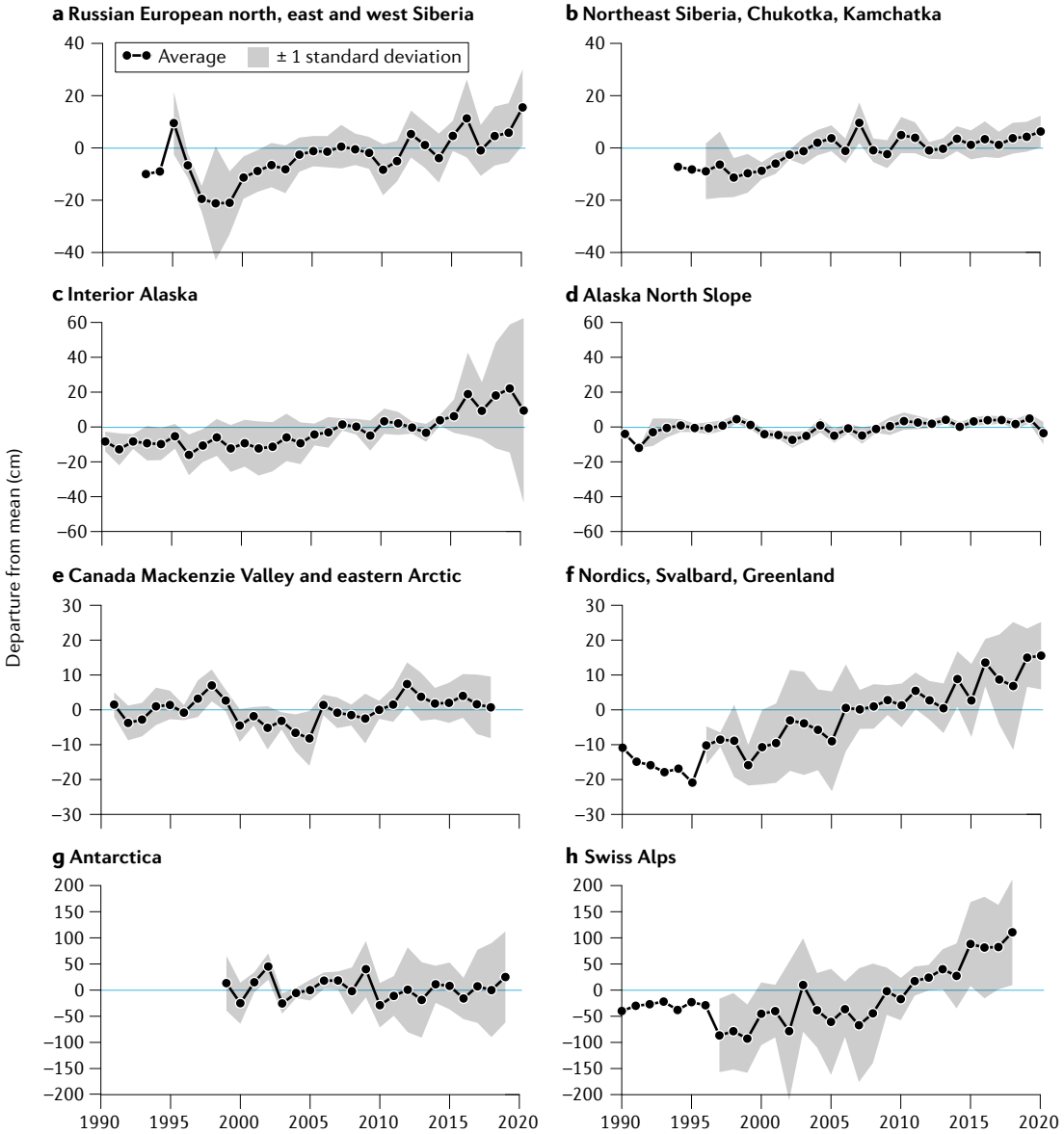

Fig. 3 | **ALT time series.** Regional average departures of active-layer thickness (ALT) from the long-term mean for European Russia, and north, east and west Siberia (panel **a**), northeast Siberia (panel **b**), interior Alaska (panel **c**), the Alaska North Slope (panel **d**), the Mackenzie Valley and eastern Arctic Canada (panel **e**), the Nordic regions, including Svalbard and Greenland (panel **f**), Antarctica (panel **g**) and the Swiss Alps (panel **h**). Data are from the CALM network. Shading denotes the standard deviation. See TABLE 1 for number of sites included in regional averages. Note the contrasting *y* axes. ALT is increasing in some regions, with change most evident at Russian, Nordic and Swiss sites.

resistivity tomography surveys can elucidate this reduction in ground ice content during permafrost degradation as temperatures rise slowly[8,26,65]. Although temperature changes in warm, ice-rich permafrost can be slow, melt of ground ice can induce substantial geomorphic changes, including ground surface subsidence and subsequent inundation, or hillslope failures[7,10]. Therefore, temperature records from warm permafrost areas do not always represent the longer-term heat flux into the permafrost and the associated geomorphic effects of climate change[62].

As discussed, there is also indication of little change in ALT at some locations despite progression of thaw deeper into the ground. This absence of ALT variability can be explained by ground surface subsidence and soil consolidation, which accompany the thaw of ice-rich permafrost. Permafrost thaw at ice-rich sites is obscured by traditional ALT measurements, which are usually made using the ground surface as the reference datum each year[66–69]. However, ground surface settlement in the range 0.2–0.8 cm per year has been observed in ice-rich terrain using differential GPS in Alaska and ground surface elevations from thaw tube measurements in the northern Mackenzie Valley[67,69]. Traditional ALT measurements therefore underestimate permafrost degradation in these regions, as lowering of the permafrost table is accompanied by subsidence of the ground surface[67]. Thus, in some situations, using ALT as an indicator of

climate change can be problematic, highlighting the need for monitoring of ground surface elevation where repeat ALT measurements are collected.

Finally, some of the variability observed in ALT records can be related to the timing of frost probe measurements. Specifically, frost probing is often performed in late summer, and thus does not always capture the period of maximum thaw, which might not occur until late October, November, or later. In addition, the length of the thaw season and timing of maximum thaw can vary from year to year. Later active-layer freeze-back due to warming and the potential for suprapermafrost talik formation also present challenges to ALT monitoring that employs probing in late summer[70]. The issue of measurement timing can be avoided by deriving ALT from continuous borehole temperature measurements, but accuracy depends on the sensor spacing and methods of interpolation or extrapolation[71].

Drivers of changes in thermal state

The response of ground temperature to changes in atmospheric conditions is modulated by the interrelated effects of vegetation, snow cover, organic layer thickness and the thermal properties of Earth material (FIG. 4), as now discussed.

Air temperature. Observed changes in permafrost thermal conditions (FIGS 1,2) are generally consistent with increases in air temperature owing to polar and high-elevation amplification[2,4,7,31,37,72]. Indeed, regional variations in the temporal patterns of air temperature are reflected in permafrost temperature records. For example, rapid warming of Canadian high-latitude Arctic permafrost since about 2000 (FIG. 2a) aligns with the rapid amplification of atmospheric temperatures that began in the late twentieth century[31,43]. By contrast, lower rates of permafrost temperature warming in the Mackenzie Valley (FIG. 2b) can be linked to smaller increases in air temperature[31,43].

Although the general patterns of air and permafrost temperature changes are coincident, local conditions prevent significant correlations (at the 95% confidence level) between the two variables[4]. For example, increases in permafrost temperature are greater at sites in bedrock, where the ground thermal conductivity is high, compared to sites underlain by unconsolidated sediments containing appreciable ground ice[8,9,19,26], where ice must thaw as temperatures rise[62]; latent heat effects in ice-rich, fine-grained sediments reduce the apparent coupling between air and ground temperatures. These effects are demonstrated at sites underlain by bedrock in Alert and Svalbard, where rates of warming are larger than those underlain by unconsolidated sediments in northwestern North America (FIGS 1,2). Similarly, in the Swiss Alps, contemporary warming is larger in ice-poor bedrock than in unconsolidated material (FIG. 2c).

The annual air temperature amplitude (difference between the warmest and the coldest months of the year), which reflects the continentality of the climate, has an important influence on ALT. For locations with the same mean annual air temperature and similar surface and soil conditions, ALT is larger in regions with a more continental climate and larger amplitude of seasonal air temperature variation[19].

The seasonality of air temperature increases is also an important factor controlling the evolution of the permafrost thermal state. In polar regions such as Alaska and northern Canada, as well as mountain regions such as the Tibetan Plateau, warming of permafrost is mainly associated with increases in winter air temperatures[72–74]. These effects are particularly marked at sites with thin snow cover[74], related to a limited buffering effect between the air and ground surface (FIG. 4). There is evidence that winter warming impacts on ALT interannual variability is also larger at Nordic sites with thin snow cover[58], although the connection with ALT is more difficult to constrain owing to the dominant impact of summer conditions on this variable.

Snow cover. Temporal variability in snow cover is an additional driver of permafrost thermal state changes owing to its insulating effect, which limits winter heat loss from the ground and modulates the influence of air temperature changes on the ground thermal regime[75]. In near-vertical bedrock slopes in the European Alps, for example, ground temperatures closely follow air temperature owing to the absence of snow cover[26,76]. The net result of an increase in snow cover is an increase in the ground surface temperature (FIG. 5a). For example, permafrost temperatures increased during periods of enhanced snow cover at monitoring sites in Alaska, even as air temperature decreased[33,73]. Late 1980s to early 1990s permafrost warming in the Alaskan interior (FIG. 2b) is further attributed to increases in both snow cover thickness and higher air temperatures[33,73]. The same factors have also been linked to permafrost warming in Norway during 1999–2009 (REF.[64]).

The magnitude of the warming effect depends on snow cover depth, timing of accumulation and melt[77],

Table 1 | **Average regional rates of ALT changes from CALM network data**

Region	Average ALT change (cm per year)[a]	Range of ALT change (cm per year)	Number of sites[b]
Alaska North Slope	0.2	−0.1–0.5	25
Alaska interior	0.9	0.2–2.7	5
Canada (Mackenzie Valley and eastern Arctic	0.0	−1.0–0.7	7
Nordic (including Svalbard and Greenland)[c]	1.3	0.5–3.8	7
Russian European north, western and central Siberia	1.3	−0.1–3.7	20
Northeastern Siberia (including Chuktoka and Kamchatka)	0.5	−0.5–1.9	24
Swiss Alps[d]	10.5	−1.8–31.6	9
Antarctica	0.1	−1.5–2.5	12

ALT, active-layer thickness. [a]ALT is determined by mechanical probing in most sites. The exceptions are Canadian sites, which use thaw tubes, and three Nordic sites and Swiss sites, which use ground-temperature measurements. [b]Sites are largely in unconsolidated material and include those with at least 10 years of data ending in 2018 or later, or after 2017 for Antarctica. [c]Two sites are in weathered bedrock with patchy till. [d]Three sites are in rock glaciers, the rest in debris slopes.

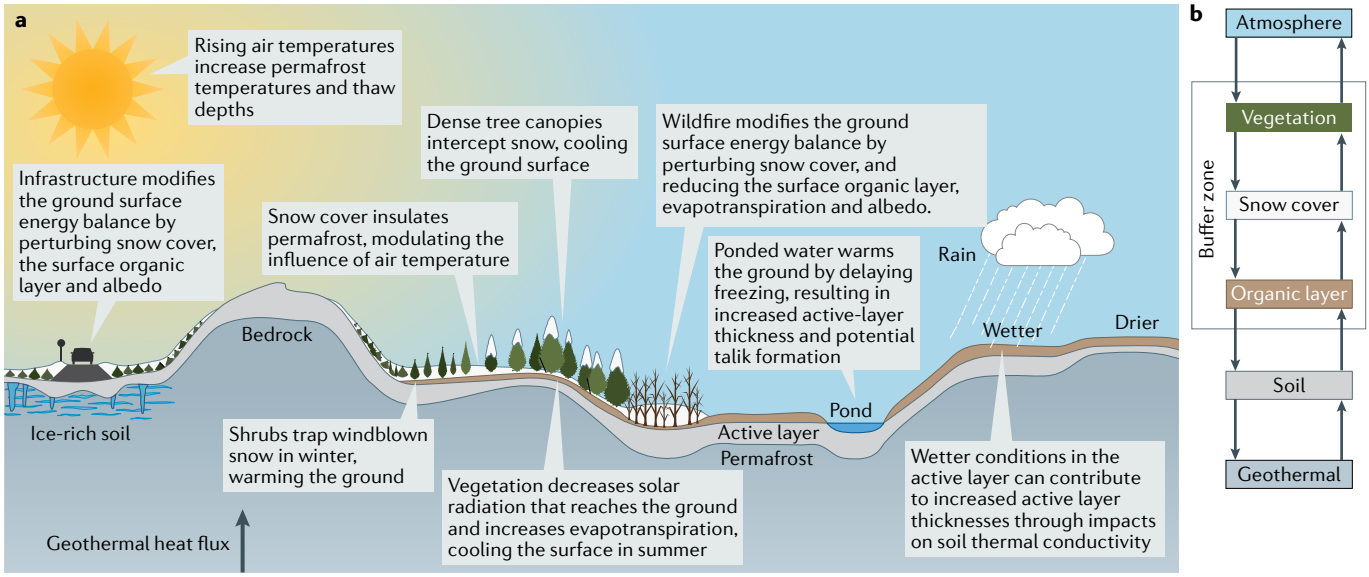

Fig. 4 | **Drivers and conditions influencing the thermal regime of permafrost.** Schematic illustration of the processes influencing active-layer thickness (panel **a**), and the key factors controlling the ground thermal regime (panel **b**). Panel **b** adapted with permission from REF.[168], Elsevier.

and snow density, all of which control the snow cover thermal properties[33]. Later accumulation can lead to enhanced cooling of the ground as air temperatures decline[77]. Thus, in the European Alps, a temporary cooling of permafrost down to depths of 20 m (FIG. 2c) was attributed to very late snow cover accumulation in two consecutive winters[26,29]. By contrast, earlier snow accumulation can delay ground cooling and freeze-back of the active layer during winter. Indeed, in the Mackenzie Delta, early snow cover accumulation led to active-layer freeze-back delays of several weeks, elevating ground temperatures compared to years in which snow accumulation occurred later[78,79]. This delay in active-layer freeze-back is larger in substrates with higher moisture content owing to latent heat release during freezing[63,79]. Timing of snow melt in spring can also influence the onset of seasonal ground warming and thaw[33,73], which will occur after the snow is gone. The warming effect also depends on the thermal properties and moisture content of the underlying soils; the greater the thermal conductivity and the higher the soil water content (and latent heat effects accompanying freezing), the larger the warming effect of the same layer of snow[63,80].

Vegetation. Vegetation also has a strong role in influencing changes in the thermal characteristics of permafrost. Yet these influences are complex owing to the interlocking effects of shading, snow accumulation and the formation of an insulating surface organic layer[73,81] (FIG. 4).

The vegetation canopy reduces the amount of solar radiation reaching the surface, decreasing summertime ground temperatures[82]. However, ground shading is spatially and temporally variable, and so the total effect on permafrost temperature is difficult to predict. For areas with dense canopies in the boreal forest, shading effects and interception of snow cover contribute to an overall cooling effect, influencing the distribution of permafrost in the discontinuous zone[81]. By contrast, enhanced snow accumulation in areas with open canopies near the treeline lead to warmer winter ground conditions[78,81]. In mid-latitude mountain regions, permafrost generally exists above the tree-line, and so vegetation is typically considered an indicator of permafrost absence[83]. Furthermore, sites with thicker organic layers are generally less responsive to changes in air temperature owing to the buffering between the air and ground surface. For example, increases in permafrost temperatures at forested sites in the central Mackenzie Valley are much lower than observed at high-latitude Arctic polar desert sites[63] (FIG. 1).

The contemporary expansion of shrubs in tundra has also been a topic of interest in regards to permafrost thermal characteristics, owing to their impact on snow cover depth. Generally, shrub presence results in warmer ground conditions compared to tundra with shorter vegetation species[78,84,85]. For example, in northwestern Canada, minimum annual near-surface ground temperatures were up to 5 °C higher at sites with tall shrubs than at sites with short shrubs[86]. While the observed expansion of shrub cover in tundra areas could therefore result in increases in permafrost temperature[85–88], direct observations of these impacts are limited.

Rainfall and soil moisture. The presence of water further has a strong impact on permafrost. Inundation leads to increases in permafrost temperature beneath the water body[89,90] because the freezing of water delays winter heat loss from the underlying ground. Taliks can form if freezing does not reach the bottom of the water body[59]. Heat advection from moving surface water (rivers, creeks, fens) can also warm the ground, resulting in permafrost degradation, particularly where the permafrost was discontinuous, warm and thin[81,91]. Thermo-erosion

associated with water flow through gullies in ice-wedge networks also leads to ground warming and increases in ALT[92]. By contrast, ground cooling occurs with emergence of the surface following pond drainage, channel migration or uplift in coastal regions[90,93,94].

Groundwater additionally affects ground temperature and ALT, specifically through the relation between soil moisture content and the thermal properties of the active layer, including thermal conductivity, heat capacity and the latent heat of freezing/thawing. Increases in water content lead to better heat conduction into the ground[95], particularly in organic soils, which combined with advective heat transfer from enhanced groundwater flow, leads to a substantial deepening of the active layer and the rapid expansion of taliks[70,82,96,97]. For organic material, the influence of moisture content on thermal conductivity is particularly apparent when comparing seasons[81,82,98,99]: drying of peat in the summer leads to lower thermal conductivity, limiting ground warming and reducing thaw penetration, whereas in autumn and winter, enhanced moisture content resulting from autumn rainfall, and its subsequent freezing, increases thermal conductivity, promoting cooling. Latent heat effects associated with evaporation from wet soils and associated surface cooling can counter the effect of increased thermal conductivity, but it is unclear whether this impact outweighs that of increased heat flow[81,95]. Moreover, latent heat effects associated with freezing of wet soils can delay freeze-back of the active layer in the autumn[81] and thaw in the spring[95]. The relation between the moisture content in the active layer and permafrost temperature is less straightforward, depending on seasonal changes to the soil's frozen and unfrozen thermal conductivity, which control the thermal offset[98,100] (BOX 1).

The infiltration of summer rainfall also influences the ground thermal regime. The magnitude of this effect depends on the difference between the soil temperature and the rain temperature, which generally approximates the air temperature[101]. Summer infiltration of water from the ground surface into the unsaturated soil of the active layer increases both ground temperature and the ALT if the rainwater is warmer than the soil[102–104], whereas rapid cooling occurs following rain events on cooler summer days or in the autumn[101]. However, knowledge of this effect comes largely from modelling, with limited field evidence of impacts of changing precipitation on the ground thermal regime[99,105]. For example, while there is some observational evidence of soil warming and accelerated spring thaw following the infiltration of rainfall[99,101,105], an insignificant correlation (at 95% confidence level) between total summer precipitation and ALT has also been observed[95]. Additional empirical evidence is required to better understand these effects, particularly the extent and significance of the process, and the direct impact of the additional energy brought by summer precipitation into the active layer[105].

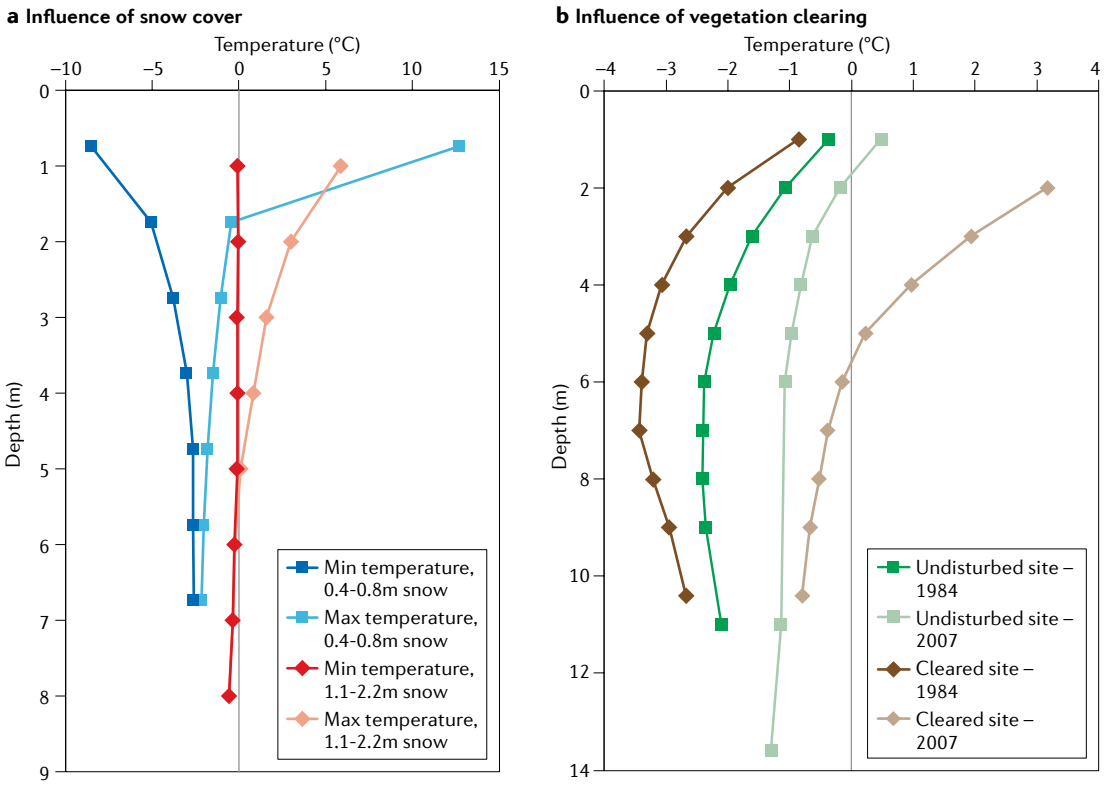

Fig. 5 | **Impact of snow and environmental disturbance on ground thermal regime.** The influence of snow cover on minimum (dark shades) and maximum (light shades) ground temperature for sites along the Dempster Highway, Canada[77] (panel **a**), where deeper snow accumulates adjacent to the embankment. The effect of vegetation clearing for a site along the pipeline right-of-way at Norman Wells, Northwest Territories, Canada (panel **b**). Higher ground temperatures and greater increases occur beneath deep snow and in sites where vegetation is cleared.

Environmental disturbances. Finally, environmental disturbances, including wildfire, human activities and thermokarst all influence thermal properties.

Wildfire is a normal occurrence in high-latitude permafrost regions, particularly in the boreal forest. However, larger and more severe fires have been observed in response to warmer and drier conditions, and fire activity is projected to increase further with continued warming[106,107]. These fires damage the protective surface organic layer that insulates the ground from warm summer air temperatures, decrease the amount of snow interception by trees, decrease the albedo at the ground surface, and decrease cooling by evapotranspiration[107–110]. Thus, ground temperatures and ALT increase following fires, with greater effects where burning is more severe and the reduction in the surface organic layer more pronounced[107,111–115]. In permafrost regions of North America, Siberia, Mongolia and northeast China[107], for example, mean annual ground surface temperatures at burned sites were 1–7 °C higher than at unburned sites.

Landscape change caused by the thaw of ice-rich permafrost (thermokarst) also influences the ground thermal regime. For example, in retrogressive thaw slumps, a type of slope failure in ice-rich permafrost, ground temperatures increase. As the vegetation mat is disturbed, ice-rich mineral soils are exposed and deep snow accumulates in the depression formed by the failure. The resulting warmer ground conditions can further enhance permafrost thaw and slumping activity[116]. Ground surface subsidence and pond formation also results in further warming of permafrost and promotion of thaw[10,117,118].

Moreover, local disturbances related to human activity disturb the ground thermal regime by altering surface conditions[118]. Structures including road, railway, runway and building embankments enhance snow accumulation, resulting in overall increases in ground temperature, ALT and permafrost degradation[77,119–121] (FIG. 5a). Clearing of vegetation and damage to the organic layer along infrastructure corridors also leads to permafrost warming beneath the cleared area (FIG. 5b) and in the adjacent undisturbed terrain due to lateral heat transfer[122,123].

Thus, several interacting drivers influence the thermal state of permafrost (FIG. 4). Air temperature and snow cover are often the dominant drivers of permafrost change, but at regional and local scales, other factors become important. Knowledge regarding the effects of some drivers, however, largely comes from modelling, motivating field-based investigations to fully understand how the permafrost thermal state will evolve in response to environmental change.

Future changes in thermal state

Given that anthropogenic warming is projected to progress, continued, or even accelerated, permafrost warming and thawing are anticipated[5,6]. The rate and pattern of these future changes will vary depending on regional climate, local environmental factors and their complex interactions[124]. As such, there is substantial uncertainty in predicting the magnitude and timing of future changes, in part, related to limitations and advantages of different modelling approaches[125].

Empirical equilibrium models. Empirically based, equilibrium models typically rely on statistical relations between the main factors driving permafrost conditions, and are thus relatively simple and require limited data input[125]. For example, models based on the frost index and temperature at the top of permafrost have been used to estimate potential future permafrost distribution at regional-to-global scales[126–130]. However, these models do not consider transient effects and cannot accurately predict the timing of permafrost loss based on imposed warming scenarios. Rather, they indicate a possible eventual (or committed) permafrost loss[127], which can lag substantially behind imposed changes in air temperature.

Estimates of eventual reductions in Northern Hemisphere permafrost area from such models range from 4.8 ± 2.0 million km^2 to 6.6 ± 2.0 million km^2 for air temperature warming scenarios of 1.5 and 2.0 °C above pre-industrial levels, respectively[127]. For the 2.0 °C scenario, the loss is equivalent to a 40% reduction of the area currently underlain by permafrost, and for the 1.5 °C scenario the reduction is 30%. Reductions >30% are similarly predicted by other simulations[129,130], with greater losses anticipated for more extreme warming scenarios. Although these results cannot accurately predict the timing of permafrost loss, they provide an estimate of areas that could undergo permafrost degradation.

In high mountain areas, permafrost distribution is highly variable and strongly driven by topography, the effect of which has been incorporated into models. The statistical relation between solar radiation (or aspect) and air temperature (or elevation) is the approach most often applied[76,131–133] and is most suitable for steep and snow-free bedrock areas. For unconsolidated material, such approaches are typically complemented by information derived from rock glacier inventories and ice-rich debris slopes[83,134]. Similar empirical approaches have been utilized to determine the future permafrost distribution in mountainous terrain in the southern Yukon, Canada[135], projecting an eventual reduction of about 50% in the area underlain by permafrost area for a 2 °C air temperature increase in the region.

Transient numerical models. Transient numerical models simulate the ground thermal regime over time[125], thus requiring detailed, site-specific input data so that heat transfer between the ground and atmosphere are accurately represented. Such models can be integrated with climate models, or incorporated in land surface or Earth System Models, to predict future ground temperatures and permafrost distribution[62,136–143]. The application of downscaled climate model outputs to drive numerical permafrost models is challenging, particularly in areas of complex topography[142,144,145]. Some simulations only focus on near-surface permafrost conditions[6,138,146,147], partly because of the computational requirements of implementing numerical models at large spatial scales to greater depths. These shallow simulations might not

accurately represent changes in the thermal state in areas of thicker, colder permafrost[148], and simulations with greater depth domains better represent the thermal response of permafrost to warming[62,140,143].

Most global-scale projections by transient models focus only on permafrost occurrence and degradation in the upper 2–3 m, rather than reductions in the total extent of permafrost[6]. From these models, predictions indicate that thaw depths will exceed 3 m in 24 ± 16% to 70 ± 20% of the current permafrost region by 2100, depending on the warming scenario[6]. Other simulations of permafrost volume change project a loss of 3.0–5.3 × 10^3 km^3 frozen material per °C atmospheric warming; thaw below 2 m depth is not considered[136].

Many models do not include representation of important subsurface properties, including excess ice content. Ground ice in excess of the soil pore space has important latent heat effects and causes ground surface subsidence upon thawing, which can strongly influence the ground thermal regime[7,149]. Neglecting such conditions is a limitation to modelling permafrost response to climate change[150], though some simulations have begun to incorporate representations of excess ice[117,151–154]. Ground ice conditions remain poorly defined in many areas, and further modelling progress will depend largely on improvements in field knowledge of ground ice conditions and improved spatial data products[155].

Realistic representation of snow cover is necessary for accurate modelling of permafrost temperatures owing to its strong insulating effect[147,156]. Snow distribution and timing have pronounced effects on ground temperatures at small spatial scales that are typically not resolved by land surface models[121,147,157]. Recent modelling shows promise in simulating snow redistribution and associated effects on ground surface temperature[158], and constitutes a novel approach for investigating climate change impacts on permafrost.

Representation of topographic effects and the spatial variability of snow cover and other important physical parameters in high-relief landscapes is an additional challenge in modelling mountain permafrost[11,83,143,159]. Numerical simulation of lateral heat fluxes in three-dimensional temperature fields are important to address changes at greater depth in steep mountain terrain[143,160]. Differential heating of mountain slopes can also substantially increase warming rates at depth in high mountain peaks or ridges[149].

Empirical and transient modelling approaches have different advantages and limitations, and it is critical to understand these capabilities to meaningfully interpret results on the extent and timing of permafrost loss. While there is high confidence that thaw depth will increase and permafrost extent will decrease, there is lower confidence in the magnitude and timing of the changes[6]. Thus, it is clear that a considerable portion of the area currently underlain by permafrost will experience varying degrees of thaw under warming.

Summary and future perspectives

Monitoring of permafrost thermal state since about 1980 provides clear evidence of warming and thawing of permafrost throughout permafrost regions. Permafrost temperatures have typically increased at a rate of around 0.2–0.8 °C per decade, with changes particularly pronounced within colder permafrost regions, including those of the continuous permafrost zone of the Arctic, and in bedrock such as at sites in the European Alps. ALT has correspondingly increased in many regions, particularly in the Russian Arctic where increases of 0.4 m are apparent over a 20-year time frame. Although changes in air temperature are a primary driver of these changes in permafrost thermal state, several other factors including snow cover and vegetation are also important. These observed trends are projected to continue in response to climate warming, albeit with large uncertainties in the magnitude and timing of changes. Indeed, although our understanding of the thermal characteristics of permafrost has developed, progress is needed in many aspects.

Permafrost is a subsurface phenomenon, meaning that monitoring relies on in situ measurements, unlike other cryospheric variables that can be measured using remote-sensing techniques. Considerable spatial gaps in monitoring networks exist, particularly in remote, less accessible areas. Additional monitoring sites in these remote areas, including in the Arctic and mountain ranges outside of Europe, are thus needed to reduce uncertainties in the characterization of permafrost thermal state worldwide. These additional ground thermal monitoring sites could benefit from robust construction and automatic data transmission[28,161]. High-quality and accessible archives with complete metadata and site information on vegetation and subsurface materials, including ground ice content, are critical for climate-related monitoring and analysis. Development of such standards will benefit from the establishment of best practices[28,161], such as those under development by Global Cryosphere Watch, to ensure standardized and comparable data sets of sufficient quality.

Remote-sensing methods could potentially also address gaps in the in situ monitoring network. Opportunities to better utilize satellite imagery for permafrost characterization have been explored[162], but available applications cannot directly monitor permafrost thermal state or ALT. However, satellite imagery analysis has been used extensively to map landscape change and ground movements associated with thawing permafrost[163–166]. These approaches provide evidence of physical changes from larger areas and complement information from ground temperature and ALT monitoring sites. Further development of applications that provide more direct measurements of important permafrost characteristics are required. For example, improved quantification of ground surface elevation and subsidence, in conjunction with thermal measurements at long-term field monitoring sites, would help to establish the extent of permafrost degradation and to reconcile measurements of subsidence with displacement measurements from satellite imagery analyses.

Simulations of future permafrost conditions predict continued warming and permafrost degradation, although there are considerable uncertainties on the magnitude and timing of changes. The relation between permafrost thermal state and climate is complex and

depends on local conditions above and below the ground surface. A greater understanding of longer-term interactions between permafrost and climate, vegetation and snow cover is required to reduce uncertainty in responses of the ground thermal regime to climate change. One example is the role of non-conductive heat transfer and the effect of summer precipitation infiltration to the active layer. Most of the knowledge related to this process has been acquired through modelling, and empirical studies are required to better assess the overall impact on permafrost temperatures. Enhancing existing permafrost monitoring sites to include additional types of observations such as air temperature, precipitation, snow cover, soil moisture and vegetation conditions would help to further elucidate relations between the various drivers as the climate changes.

The field-based research suggested here would contribute to improved model representation of interactions between hydrologic processes and geomorphic (landscape) and permafrost conditions, and would reduce uncertainties in projections. Updated information on ground ice conditions is required for model input, and validation with field measurements is needed to ensure reasonable process representation in simulations.

Published online 11 January 2022

1. Harris, S. A. et al. *Glossary of Permafrost and Related Ground-Ice Terms* Vol. 154 (National Research Council Canada, 1988).
2. Wang, Q., Fan, X. & Wang, M. Recent warming amplification over high elevation regions across the globe. *Clim. Dyn.* **43**, 87–101 (2014).
3. Serreze, M. C. & Barry, R. G. Processes and impacts of Arctic amplification: a research synthesis. *Glob. Planet. Change* **77**, 85–96 (2011).
4. Biskaborn, B. K. et al. Permafrost is warming at a global scale. *Nat. Commun.* **10**, 1–11 (2019).
5. Derksen, C. et al. in *Canada's Changing Climate Report* Ch. 5 (eds Bush, E. & Lemmen, D. S.) 194–260 (Government of Canada, 2019).
6. Intergovernmental Panel on Climate Change. Special report on the ocean and cryosphere in a changing climate (IPCC, 2019).
7. Romanovsky, V. E. et al. in *Snow, Water, Ice and Permafrost in the Arctic (SWIPA) 2017* Ch. 4 65–102 (AMAP, 2017).
8. Etzelmüller, B. et al. Twenty years of European mountain permafrost dynamics — the PACE legacy. *Environ. Res. Lett.* **15**, 104070 (2020).
9. Haberkorn, A., Kenner, R., Noetzli, J. & Phillips, M. Changes in ground temperature and dynamics in mountain permafrost in the Swiss Alps. *Front. Earth Sci.* **9**, 626686 (2021).
10. Kokelj, S. V. & Jorgenson, M. T. Advances in thermokarst research. *Permafr. Periglac. Process.* **24**, 108–119 (2013).
11. Gruber, S. & Haeberli, W. Permafrost in steep bedrock slopes and its temperature-related destabilization following climate change. *J. Geophys. Res.* **112**, F02S18 (2007).
12. Marcer, M. et al. Rock glaciers throughout the French Alps accelerated and destabilised since 1990 as air temperatures increased. *Commun. Earth Environ.* **2**, 81 (2021).
13. Krautblatter, M., Funk, D. & Günzel, F. K. Why permafrost rocks become unstable: a rock-ice-mechanical model in time and space. *Earth Surf. Process. Landf.* **38**, 876–887 (2013).
14. Bommer, C., Phillips, M. & Arenson, L. U. Practical recommendations for planning, constructing and maintaining infrastructure in mountain permafrost: mountain Infrastructure. *Permafr. Periglac. Process.* **21**, 97–104 (2010).
15. Hjort, J. et al. Impacts of permafrost degradation on infrastructure. *Nat. Rev. Earth Environ.* https://doi.org/10.1038/s43017-021-00247-8 (2021).
16. Hugelius, G. et al. Estimated stocks of circumpolar permafrost carbon with quantified uncertainty ranges and identified data gaps. *Biogeosciences* **11**, 6573–6593 (2014).
17. Miner, K. R. et al. Permafrost carbon emissions in a changing Arctic. *Nat. Rev. Earth Environ.* https://doi.org/10.1038/s43017-021-00230-3 (2021).
18. Biskaborn, B. K. et al. The new database of the Global Terrestrial Network for Permafrost (GTN-P). *Earth Syst. Sci. Data* **7**, 245–259 (2015).
19. Romanovsky, V. E., Smith, S. L. & Christiansen, H. H. Permafrost thermal state in the polar Northern Hemisphere during the international polar year 2007–2009: a synthesis. *Permafr. Periglac. Process.* **21**, 106–116 (2010).
20. Harris, C., Haeberli, W., Vonder Mühll, D. & King, L. Permafrost monitoring in the high mountains of Europe: the PACE Project in its global context. *Permafr. Periglac. Process.* **12**, 3–11 (2001).
21. Harris, C. et al. Permafrost and climate in Europe: monitoring and modelling thermal, geomorphological and geotechnical responses. *Earth Sci. Rev.* **92**, 117–171 (2009).
22. Vieira, G. et al. Thermal state of permafrost and active-layer monitoring in the Antarctic: advances during the international polar year 2007–2009. *Permafr. Periglac. Process.* **21**, 182–197 (2010).
23. Zhao, L., Wu, Q., Marchenko, S. S. & Sharkhuu, N. Thermal state of permafrost and active layer in Central Asia during the international polar year. *Permafr. Periglac. Process.* **21**, 198–207 (2010).
24. Brown, J., Hinkel, K. M. & Nelson, F. E. The Circumpolar Active Layer Monitoring (CALM) program: research designs and initial results. *Polar Geogr.* **24**, 166–258 (2000).
25. Duchesne, C., Smith, S. L., Ednie, M. & Bonnaventure, P. P. in *Proc. 68th Canadian Geotechnical Conf. 7th Canadian Permafrost Conf.* (Canadian Geotechnical Society, 2015).
26. Swiss Permafrost Monitoring Network. Permafrost in Switzerland 2014/2015 to 2017/2018 (PERMOS, 2019).
27. Smith, S. L. & Brown, J. Assessment of the status of the development of the standards for the Terrestrial Essential Climate Variables — T7 — Permafrost and seasonally frozen ground (GTOS, 2009).
28. Noetzli, J. et al. Best practice for measuring permafrost temperature in boreholes based on the experience in the Swiss Alps. *Front. Earth Sci.* **9**, 607875 (2021).
29. Noetzli, J. et al. State of the climate in 2019. *Bull. Am. Met. Soc.* **101**, S34–S36 (2020).
30. Romanovsky, V. E. et al. State of the climate in 2019. *Bull. Am. Met. Soc.* **101**, S265–S269 (2020).
31. Smith, S. L., Duchesne, C. & Lewkowicz, A. G. in *Cold Regions Engineering 2019* (eds Bilodeau, J. P., Nadeau, D. F., Fortier, D. & Conciatori, D.) 670–677 (American Society of Civil Engineers, 2019).
32. Zhao, L. et al. Changing climate and the permafrost environment on the Qinghai–Tibet (Xizang) plateau. *Permafr. Periglac. Process.* **31**, 396–405 (2020).
33. Osterkamp, T. E. in *Proc. Ninth Int. Conf. Permafrost* Vol. 2 (eds Kane, D. L. & Hinkel, K. M.) 1333–1338 (Inst. Northern Engineering, Univ. Alaska, 2008).
34. Smith, S. L., Burgess, M. M. & Taylor, A. E. in *Permafrost: Proc. 8th Int. Conf. Permafrost* (eds Phillips, M., Springman, S. M. & Arenson, L. U.) 1073–1078 (CRC, 2003).
35. Smith, S. L., Burgess, M. M., Riseborough, D. & Nixon, F.M. Recent trends from Canadian permafrost thermal monitoring network sites. *Permafr. Periglac. Process.* **16**, 19–30 (2005).
36. Allard, M., Wang, B. & Pilon, J. Recent cooling along the southern shore of Hudson Strait, Quebec, Canada, documented from permafrost temperature measurements. *Arctic Antarctic Alp. Res.* **27**, 157–166 (1995).
37. Romanovsky, V. E., Sazonova, T. S., Balobaev, V. T., Shender, N. I. & Sergueev, D. O. Past and recent changes in air and permafrost temperatures in eastern Siberia. *Glob. Planet. Change* **56**, 399–413 (2007).
38. Harris, C. et al. Warming permafrost in European mountains. *Glob. Planet. Change* **39**, 215–225 (2003).
39. Isaksen, K., Sollid, J. L., Holmlund, P. & Harris, C. Recent warming of mountain permafrost in Svalbard and Scandinavia. *J. Geophys. Res.* **112**, F02S04 (2007).
40. Wu, Q. & Zhang, T. Recent permafrost warming on the Qinghai–Tibetan Plateau. *J. Geophys. Res.* **113**, D13108 (2008).
41. Christiansen, H. H. et al. The thermal state of permafrost in the Nordic area during the international polar year 2007–2009. *Permafr. Periglac. Process.* **21**, 156–181 (2010).
42. Romanovsky, V. E. et al. Thermal state of permafrost in Russia. *Permafr. Periglac. Process.* **21**, 136–155 (2010).
43. Smith, S. et al. Thermal state of permafrost in North America: a contribution to the international polar year. *Permafr. Periglac. Process.* **21**, 117–135 (2010).
44. Duchesne, C., Chartrand, J. & Smith, S. L. Report on 2018 field activities and collection of ground-thermal and active-layer data in the Mackenzie Corridor, Northwest Territories (Natural Resources Canada, 2020).
45. Allard, M., Sarrazin, D. & L'Hérault, E. Borehole and near-surface ground temperatures in Northeastern Canada. *Nordicana D* https://doi.org/10.5885/45291SL-34F28A9491014AFD (2020).
46. Drozdov, D. S. et al. in *Proc. 68th Canadian Geotechnical Conf. 7th Canadian Permafrost Conf.* (Canadian Geotechnical Society, 2015).
47. Vasiliev, A. A. et al. Permafrost degradation in the Western Russian Arctic. *Environ. Res. Lett.* **15**, 045001 (2020).
48. Noetzli, J. et al. State of the climate in 2018. *Bull. Am. Met. Soc.* **100**, S21–S22 (2019).
49. Schmid, M.-O. et al. Assessment of permafrost distribution maps in the Hindu Kush Himalayan region using rock glaciers mapped in Google Earth. *Cryosphere* **9**, 2089–2099 (2015).
50. Allen, S. K. et al. Permafrost studies in Kullu District, Himachal Pradesh. *Curr. Sci.* **111**, 550 (2016).
51. Hasler, A., Geertsema, M., Foord, V., Gruber, S. & Noetzli, J. The influence of surface characteristics, topography and continentality on mountain permafrost in British Columbia. *Cryosphere* **9**, 1025–1038 (2015).
52. Gruber, S. et al. in *Proc. 68th Canadian Geotechnical Conf. 7th Canadian Permafrost Conf.* (Canadian Geotechnical Society, 2015).
53. Andrés, N., Palacios, D., Úbeda, J. & Alcalá, J. Ground thermal conditions at Chachani volcano, southern Peru. *Geograf. Ann. Ser. A* **93**, 151–162 (2011).
54. Nagy, B., Ignéczi, Á., Kovács, J., Szalai, Z. & Mari, L. Shallow ground temperature measurements on the highest volcano on Earth, Mt. Ojos del Salado, Arid Andes, Chile. *Permafr. Periglac. Process.* **30**, 3–18 (2019).
55. Yoshikawa, K. et al. Current thermal state of permafrost in the southern Peruvian Andes and potential impact from El Niño–Southern Oscillation (ENSO). *Permafr. Periglac. Process.* **31**, 598–609 (2020).
56. Allen, S. K., Gruber, S. & Owens, I. F. Exploring steep bedrock permafrost and its relationship with recent slope failures in the southern Alps of New Zealand. *Permafr. Periglac. Process.* **20**, 345–356 (2009).
57. Abramov, A. et al. Two decades of active layer thickness monitoring in northeastern Asia. *Polar Geogr.* https://doi.org/10.1080/1088937X.2019.1648581 (2019).
58. Strand, S. M., Christiansen, H. H., Johansson, M., Åkerman, J. & Humlum, O. Active layer thickening and controls on interannual variability in the Nordic Arctic compared to the circum-Arctic. *Permafr. Periglac. Process.* **32**, 47–58 (2021).
59. O'Neill, H. B., Roy-Leveillee, P., Lebedeva, L. & Ling, F. Recent advances (2010–2019) in the study of taliks. *Permafrost Periglac Process* **31**, 346–357 (2020).

60. Hrbáček, F. et al. Active layer monitoring in Antarctica: an overview of results from 2006 to 2015. *Polar Geogr.* https://doi.org/10.1080/1088937X.2017.1420105 (2018).
61. Ramos, M. et al. Recent shallowing of the thaw depth at Crater Lake, Deception Island, Antarctica (2006–2014). *CATENA* **149**, 519–528 (2017).
62. Nicolsky, D. J. & Romanovsky, V. E. Modeling long-term permafrost degradation. *J. Geophys. Res. Earth Surf.* **123**, 1756–1771 (2018).
63. Throop, J., Lewkowicz, A. G. & Smith, S. L. Climate and ground temperature relations at sites across the continuous and discontinuous permafrost zones, northern Canada. *Can. J. Earth Sci.* **49**, 865–876 (2012).
64. Isaksen, K. et al. Degrading mountain permafrost in southern Norway: spatial and temporal variability of mean ground temperatures, 1999–2009. *Permafr. Periglac. Process.* **22**, 361–377 (2011).
65. Mollaret, C. et al. Mountain permafrost degradation documented through a network of permanent electrical resistivity tomography sites. *Cryosphere* **13**, 2557–2578 (2019).
66. Farquharson, L. M. et al. Climate change drives widespread and rapid thermokarst development in very cold permafrost in the Canadian high Arctic. *Geophys. Res. Lett.* **46**, 6681–6689 (2019).
67. O'Neill, H. B., Smith, S. L. & Duchesne, C. in *Cold Regions Engineering 2019* (eds Bilodeau, J. P., Nadeau, D. F., Fortier, D. & Conciatori, D.) 643–651 (American Society of Civil Engineers, 2019).
68. Shiklomanov, N. I., Streletskiy, D. A., Little, J. D. & Nelson, F. E. Isotropic thaw subsidence in undisturbed permafrost landscapes. *Geophys. Res. Lett.* **40**, 6356–6361 (2013).
69. Streletskiy, D. A. et al. Thaw subsidence in undisturbed tundra landscapes, Barrow, Alaska, 1962–2015: Barrow subsidence. *Permafr. Periglac. Process.* **28**, 566–572 (2017).
70. Connon, R., Devoie, É., Hayashi, M., Veness, T. & Quinton, W. The influence of shallow taliks on permafrost thaw and active layer dynamics in subarctic Canada. *J. Geophys. Res. Earth Surf.* **123**, 281–297 (2018).
71. Riseborough, D. W. in *Proc. Ninth Int. Conf. Permafrost* Vol. 2 (eds Kane, D. L. & Hinkel, K. M.) 1487–1492 (Inst. Northern Engineering, Univ. Alaska, 2008).
72. Zhang, G., Nan, Z., Wu, X., Ji, H. & Zhao, S. The role of winter warming in permafrost change over the Qinghai–Tibet plateau. *Geophys. Res. Lett.* **46**, 11261–11269 (2019).
73. Osterkamp, T. E. Characteristics of the recent warming of permafrost in Alaska. *J. Geophys. Res.* **112**, F02S02 (2007).
74. Smith, S. L., Throop, J., Lewkowicz, A. G. & Burn, C. R. Recent changes in climate and permafrost temperatures at forested and polar desert sites in northern Canada. *Can. J. Earth Sci.* **49**, 914–924 (2012).
75. Taylor, A. E., Wang, K., Smith, S. L., Burgess, M. M. & Judge, A. S. Canadian Arctic Permafrost Observatories: detecting contemporary climate change through inversion of subsurface temperature time series. *J. Geophys. Res.* **111**, 1–14 (2006).
76. Gruber, S., Hoelzle, M. & Haeberli, W. Rock-wall temperatures in the Alps: modelling their topographic distribution and regional differences. *Permafr. Periglac. Process.* **15**, 299–307 (2004).
77. O'Neill, H. B. & Burn, C. R. Impacts of variations in snow cover on permafrost stability, including simulated snow management, Dempster Highway, Peel Plateau, Northwest Territories. *Arct. Sci.* **3**, 150–178 (2017).
78. Palmer, M. J., Burn, C. R., Kokelj, S. V. & Allard, M. Factors influencing permafrost temperatures across tree line in the uplands east of the Mackenzie Delta, 2004–2010. *Can. J. Earth Sci.* **49**, 877–894 (2012).
79. Morse, P. D., Burn, C. R. & Kokelj, S. V. Influence of snow on near-surface ground temperatures in upland and alluvial environments of the outer Mackenzie Delta, Northwest Territories. *Can. J. Earth Sci.* **49**, 895–913 (2012).
80. Sazonova, T. S. & Romanovsky, V. E. A model for regional-scale estimation of temporal and spatial variability of active layer thickness and mean annual ground temperatures. *Permafr. Periglac. Process.* **14**, 125–139 (2003).
81. Loranty, M. M. et al. Reviews and syntheses: Changing ecosystem influences on soil thermal regimes in northern high-latitude permafrost regions. *Biogeosciences* **15**, 5287–5313 (2018).
82. Juszak, I., Eugster, W., Heijmans, M. M. P. D. & Schaepman-Strub, G. Contrasting radiation and soil heat fluxes in Arctic shrub and wet sedge tundra. *Biogeosciences* **13**, 4049–4064 (2016).
83. Boeckli, L., Brenning, A., Gruber, S. & Noetzli, J. A statistical approach to modelling permafrost distribution in the European Alps or similar mountain ranges. *Cryosphere* **6**, 125–140 (2012).
84. Burn, C. R. & Kokelj, S. V. The environment and permafrost of the Mackenzie Delta area. *Permafr. Periglac. Process.* **20**, 83–105 (2009).
85. Kropp, H. et al. Shallow soils are warmer under trees and tall shrubs across Arctic and boreal ecosystems. *Environ. Res. Lett.* **16**, 015001 (2020).
86. Lantz, T. C., Marsh, P. & Kokelj, S. V. Recent shrub proliferation in the mackenzie delta uplands and microclimatic implications. *Ecosystems* **16**, 47–59 (2013).
87. Frost, G. V., Epstein, H. E., Walker, D. A., Matyshak, G. & Ermokhina, K. Seasonal and long-term changes to active-layer temperatures after tall shrubland expansion and succession in Arctic tundra. *Ecosystems* **21**, 507–520 (2018).
88. Myers-Smith, I. H. et al. Climate sensitivity of shrub growth across the tundra biome. *Nat. Clim. Chang.* **5**, 887–891 (2015).
89. Boike, J. et al. Thermal processes of thermokarst lakes in the continuous permafrost zone of northern Siberia — observations and modeling (Lena River Delta, Siberia). *Biogeosciences* **12**, 5941–5965 (2015).
90. Jones, B. M. et al. Increase in beaver dams controls surface water and thermokarst dynamics in an Arctic tundra region, Baldwin Peninsula, northwestern Alaska. *Environ. Res. Lett.* **15**, 075005 (2020).
91. Quinton, W. et al. A synthesis of three decades of hydrological research at Scotty Creek, NWT, Canada. *Hydrol. Earth Syst. Sci.* **23**, 2015–2039 (2019).
92. Godin, E. & Fortier, D. Geomorphology of a thermo-erosion gully, Bylot Island, Nunavut, Canada. *Can. J. Earth Sci.* **49**, 979–986 (2012).
93. Boisson, A., Allard, M. & Sarrazin, D. Permafrost aggradation along the emerging eastern coast of Hudson Bay, Nunavik (northern Québec, Canada). *Permafr. Periglac. Process.* **31**, 128–140 (2020).
94. Mackay, J. R. & Burn, C. R. The first 20 years (1978–1979 to 1998–1999) of ice-wedge growth at the Illisarvik experimental drained lake site, western Arctic coast, Canada. *Can. J. Earth Sci.* **39**, 95–111 (2002).
95. Clayton, L. K. et al. Active layer thickness as a function of soil water content. *Environ. Res. Lett.* **16**, 055028 (2021).
96. Wright, N., Hayashi, M. & Quinton, W. L. Spatial and temporal variations in active layer thawing and their implication on runoff generation in peat-covered permafrost terrain. *Water Resour. Res.* **45**, 1–13 (2009).
97. Devoie, É. G., Craig, J. R., Connon, R. F. & Quinton, W. L. Taliks: a tipping point in discontinuous permafrost degradation in peatlands. *Water Resour. Res.* **55**, 9838–9857 (2019).
98. Romanovsky, V. E. & Osterkamp, T. E. Interannual variations of the thermal regime of the active layer and near-surface permafrost in northern Alaska. *Permafr. Periglac. Process.* **6**, 313–335 (1995).
99. Douglas, T. A., Turetsky, M. R. & Koven, C. D. Increased rainfall stimulates permafrost thaw across a variety of Interior Alaskan boreal ecosystems. *npj Clim. Atmos. Sci.* **3**, 28 (2020).
100. Burn, C. R. & Smith, C. A. S. Observations of the 'thermal offset' in near-surface mean annual ground temperatures at several sites near Mayo, Yukon Territory, Canada. *Arctic* **41**, 99–104 (1988).
101. Neumann, R. B. et al. Warming effects of spring rainfall increase methane emissions from thawing permafrost. *Geophys. Res. Lett.* **46**, 1393–1401 (2019).
102. Guan, X. J., Spence, C. & Westbrook, C. J. Shallow soil moisture — ground thaw interactions and controls — Part 2: Influences of water and energy fluxes. *Hydrol. Earth Syst. Sci.* **14**, 1387–1400 (2010).
103. Zhang, Y. et al. Comparison of algorithms and parameterisations for infiltration into organic-covered permafrost soils. *Hydrol. Earth Syst. Sci.* **14**, 729–750 (2010).
104. Grant, R. F., Humphreys, E. R. & Lafleur, P. M. Ecosystem CO_2 and CH_4 exchange in a mixed tundra and a fen within a hydrologically diverse Arctic landscape: 1. Modeling versus measurements: CO_2 and CH_4 exchange in the Arctic. *J. Geophys. Res. Biogeosci.* **120**, 1366–1387 (2015).
105. Mekonnen, Z. A., Riley, W. J., Grant, R. F. & Romanovsky, V. E. Changes in precipitation and air temperature contribute comparably to permafrost degradation in a warmer climate. *Environ. Res. Lett.* **16**, 024008 (2021).
106. Flannigan, M. et al. Global wildland fire season severity in the 21st century. *For. Ecol. Manag.* **294**, 54–61 (2013).
107. Holloway, J. E. et al. Impact of wildfire on permafrost landscapes: a review of recent advances and future prospects. *Permafr. Periglac. Process.* **31**, 371–382 (2020).
108. Jones, B. M. et al. Recent Arctic tundra fire initiates widespread thermokarst development. *Sci. Rep.* **5**, 15865 (2015).
109. Viereck, L. A. in *Proc. 4th Canadian Permafrost Conf.* (ed. French, H. M.) 123–135 (National Research Council of Canada, 1982).
110. Burn, C. R. in *Cryosols: Permafrost-Affected Soils* (ed. Kimble, J. M.) 391–413 (Springer, 2004).
111. Brown, D. R. N. et al. Interactive effects of wildfire and climate on permafrost degradation in Alaskan lowland forests. *J. Geophys. Res. Biogeosci.* **120**, 1619–1637 (2015).
112. Kirdyanov, A. V. et al. Long-term ecological consequences of forest fires in the continuous permafrost zone of Siberia. *Environ. Res. Lett.* **15**, 034061 (2020).
113. Li, X. et al. Effects of forest fires on the permafrost environment in the northern Da Xing'anling (Hinggan) mountains, northeast China. *Permafr. Periglac. Process.* **30**, 163–177 (2019).
114. Narita, K. et al. Vegetation and permafrost thaw depth 10 years after a tundra fire in 2002, Seward Peninsula, Alaska. *Arctic Antarctic Alp. Res.* **47**, 547–559 (2015).
115. Smith, S. L., Riseborough, D. W. & Bonnaventure, P. P. Eighteen year record of forest fire effects on ground thermal regimes and permafrost in the central Mackenzie Valley, NWT, Canada. *Permafr. Periglac. Process.* **26**, 289–303 (2015).
116. Kokelj, S. V., Lantz, T. C., Kanigan, J., Smith, S. L. & Coutts, R. Origin and polycyclic behaviour of tundra thaw slumps, Mackenzie Delta region, Northwest Territories, Canada. *Permafr. Periglac. Process.* **20**, 173–184 (2009).
117. Nitzbon, J. et al. Fast response of cold ice-rich permafrost in northeast Siberia to a warming climate. *Nat. Commun.* **11**, 2201 (2020).
118. Raynolds, M. K. et al. Cumulative geoecological effects of 62 years of infrastructure and climate change in ice-rich permafrost landscapes, Prudhoe Bay Oilfield, Alaska. *Glob. Change Biol.* **20**, 1211–1224 (2014).
119. Hinkel, K. M. & Hurd, J. K. Jr Permafrost destabilization and thermokarst following snow fence installation, Barrow, Alaska, U.S.A. *Arctic Antarctic Alp. Res.* **38**, 530–539 (2006).
120. Johansson, M. et al. Rapid responses of permafrost and vegetation to experimentally increased snow cover in sub-Arctic Sweden. *Environ. Res. Lett.* **8**, 035025 (2013).
121. O'Neill, H. B. & Burn, C. R. Talik formation at a snow fence in continuous permafrost, western Arctic Canada. *Permafr. Periglac. Process.* **28**, 558–565 (2017).
122. Smith, S. L., Burgess, M. M. & Riseborough, D. W. in *Proc. Ninth Int. Conf. Permafrost* Vol. 2 (eds Kane, D. L. & Hinkel, K. M.) 1665–1670 (Inst. Northern Engineering, Univ. Alaska, 2008).
123. Smith, S. L. & Riseborough, D. W. Modelling the thermal response of permafrost terrain to right-of-way disturbance and climate warming. *Cold Reg. Sci. Technol.* **60**, 92–103 (2010).
124. Fisher, R. A. & Koven, C. D. Perspectives on the future of land surface models and the challenges of representing complex terrestrial systems. *J. Adv. Model. Earth Syst.* **12**, e2018MS001453 (2020).
125. Riseborough, D. W., Shiklomanov, N., Etzelmüller, B., Gruber, S. & Marchenko, S. Recent advances in permafrost modelling. *Permafr. Periglac. Process.* **19**, 137–156 (2008).
126. Aalto, J., Karjalainen, O., Hjort, J. & Luoto, M. Statistical forecasting of current and future circum-Arctic ground temperatures and active layer thickness. *Geophys. Res. Lett.* **45**, 4889–4898 (2018).
127. Chadburn, S. E. et al. An observation-based constraint on permafrost loss as a function of global warming. *Nat. Clim. Chang.* **7**, 340–344 (2017).
128. Farbrot, H., Isaksen, K., Etzelmüller, B. & Gisnås, K. Ground thermal regime and permafrost distribution under a changing climate in northern Norway. *Permafr. Periglac. Process.* **24**, 20–38 (2013).
129. Guo, D. & Wang, H. CMIP5 permafrost degradation projection: a comparison among different regions. *J. Geophys. Res. Atmos.* **121**, 4499–4517 (2016).

130. Kong, Y. & Wang, C.-H. Responses and changes in the permafrost and snow water equivalent in the Northern Hemisphere under a scenario of 1.5 °C warming. *Adv. Clim. Chang. Res.* **8**, 235–244 (2017).
131. Etzelmüller, B. et al. Mapping and modelling the occurrence and distribution of mountain permafrost. *Nor. Geografisk Tidsskr. Nor. J. Geogr.* **55**, 186–194 (2001).
132. Noetzli, J., Hoelzle, M. & Haeberli, W. in *Permafrost: Proc. 8th Int. Conf. Permafrost* (eds Phillips, M., Springman, S. M. & Arenson, L. U.) 827–832 (CRC, 2003).
133. Gruber, S. Derivation and analysis of a high-resolution estimate of global permafrost zonation. *Cryosphere* **6**, 221–233 (2012).
134. Kenner, R., Noetzli, J., Hoelzle, M., Raetzo, H. & Phillips, M. Distinguishing ice-rich and ice-poor permafrost to map ground temperatures and ground ice occurrence in the Swiss Alps. *Cryosphere* **13**, 1925–1941 (2019).
135. Bonnaventure, P. P. & Lewkowicz, A. G. Impacts of mean annual air temperature change on a regional permafrost probability model for the southern Yukon and northern British Columbia, Canada. *Cryosphere* **7**, 935–946 (2013).
136. Burke, E. J., Zhang, Y. & Krinner, G. Evaluating permafrost physics in the Coupled Model Intercomparison Project 6 (CMIP6) models and their sensitivity to climate change. *Cryosphere* **14**, 3155–3174 (2020).
137. Qin, Y. et al. Numerical modeling of the active layer thickness and permafrost thermal state across Qinghai–Tibetan plateau. *J. Geophys. Res. Atmos.* **122**, 11,604–11,620 (2017).
138. Slater, A. G. & Lawrence, D. M. Diagnosing present and future permafrost from climate models. *J. Clim.* **26**, 5608–5623 (2013).
139. Westermann, S., Schuler, T. V., Gisnås, K. & Etzelmüller, B. Transient thermal modeling of permafrost conditions in southern Norway. *Cryosphere* **7**, 719–739 (2013).
140. Zhang, Y., Chen, W. & Riseborough, D. W. Transient projections of permafrost distribution in Canada during the 21st century under scenarios of climate change. *Glob. Planet. Change* **60**, 443–456 (2008).
141. Marmy, A., Salzmann, N., Scherler, M. & Hauck, C. Permafrost model sensitivity to seasonal climatic changes and extreme events in mountainous regions. *Environ. Res. Lett.* **8**, 035048 (2013).
142. Fiddes, J. & Gruber, S. TopoSUB: a tool for efficient large area numerical modelling in complex topography at sub-grid scales. *Geosci. Model. Dev.* **5**, 1245–1257 (2012).
143. Noetzli, J., Gruber, S., Kohl, T., Salzmann, N. & Haeberli, W. Three-dimensional distribution and evolution of permafrost temperatures in idealized high-mountain topography. *J. Geophys. Res.* **112**, F02S13 (2007).
144. Salzmann, N., Frei, C., Vidale, P.-L. & Hoelzle, M. The application of Regional Climate Model output for the simulation of high-mountain permafrost scenarios. *Glob. Planet. Change* **56**, 188–202 (2007).
145. Marmy, A. et al. Semi-automated calibration method for modelling of mountain permafrost evolution in Switzerland. *Cryosphere* **10**, 2693–2719 (2016).
146. Koven, C. D., Riley, W. J. & Stern, A. Analysis of permafrost thermal dynamics and response to climate change in the CMIP5 Earth System Models. *J. Clim.* **26**, 1877–1900 (2013).
147. Pruessner, L., Phillips, M., Farinotti, D., Hoelzle, M. & Lehning, M. Near-surface ventilation as a key for modeling the thermal regime of coarse blocky rock glaciers. *Permafr. Periglac. Process.* **29**, 152–163 (2018).
148. Burn, C. R. & Nelson, F. E. Comment on "A projection of severe near-surface permafrost degradation during the 21st century" by David M. Lawrence and Andrew G. Slater. *Geophys. Res. Lett.* **33**, L21503 (2006).
149. Noetzli, J. & Gruber, S. Transient thermal effects in Alpine permafrost. *Cryosphere* **3**, 85–99 (2009).
150. O'Neill, H. B. et al. Permafrost thaw and northern development. *Nat. Clim. Chang.* **10**, 722–723 (2020).
151. Aas, K. S. et al. Thaw processes in ice-rich permafrost landscapes represented with laterally coupled tiles in a land surface model. *Cryosphere* **13**, 591–609 (2019).
152. Cai, L., Lee, H., Aas, K. S. & Westermann, S. Projecting circum-Arctic excess-ground-ice melt with a sub-grid representation in the Community Land Model. *Cryosphere* **14**, 4611–4626 (2020).
153. Lee, H., Swenson, S. C., Slater, A. G. & Lawrence, D. M. Effects of excess ground ice on projections of permafrost in a warming climate. *Environ. Res. Lett.* **9**, 124006 (2014).
154. Westermann, S. et al. Simulating the thermal regime and thaw processes of ice-rich permafrost ground with the land-surface model CryoGrid 3. *Geosci. Model. Dev.* **9**, 523–546 (2016).
155. O'Neill, H. B., Wolfe, S. A. & Duchesne, C. New ground ice maps for Canada using a paleogeographic modelling approach. *Cryosphere* **13**, 753–773 (2019).
156. Wang, Q., Fan, X. & Wang, M. Evidence of high-elevation amplification versus Arctic amplification. *Sci. Rep.* **6**, 19219 (2016).
157. Gisnås, K. et al. A statistical approach to represent small-scale variability of permafrost temperatures due to snow cover. *Cryosphere* **8**, 2063–2074 (2014).
158. Zweigel, R. B. et al. Simulating snow redistribution and its effect on ground surface temperature at a high-arctic site on svalbard. *J. Geophys. Res. Earth Surf.* **126**, e2020JF005673 (2021).
159. Fiddes, J., Aalstad, K. & Westermann, S. Hyper-resolution ensemble-based snow reanalysis in mountain regions using clustering. *Hydrol. Earth Syst. Sci.* **23**, 4717–4736 (2019).
160. Magnin, F. et al. Modelling rock wall permafrost degradation in the Mont Blanc massif from the LIA to the end of the 21st century. *Cryosphere* **11**, 1813–1834 (2017).
161. Steffen, K. & Box, J. Surface climatology of the Greenland Ice Sheet: Greenland Climate Network 1995–1999. *J. Geophys. Res.* **106**, 33951–33964 (2001).
162. National Research Council. Opportunities to use remote sensing in understanding permafrost and related ecological characteristics: report of a workshop (National Academies Press, 2014).
163. Chen, J., Günther, F., Grosse, G., Liu, L. & Lin, H. Sentinel-1 InSAR measurements of elevation changes over Yedoma Uplands on Sobo-Sise Island, Lena Delta. *Remote. Sens.* **10**, 1152 (2018).
164. Lewkowicz, A. G. & Way, R. G. Extremes of summer climate trigger thousands of thermokarst landslides in a High Arctic environment. *Nat. Commun.* **10**, 1329 (2019).
165. Liljedahl, A. K. et al. Pan-Arctic ice-wedge degradation in warming permafrost and its influence on tundra hydrology. *Nat. Geosci.* **9**, 312–318 (2016).
166. Rouyet, L., Lauknes, T. R., Christiansen, H. H., Strand, S. M. & Larsen, Y. Seasonal dynamics of a permafrost landscape, Adventdalen, Svalbard, investigated by InSAR. *Remote Sens. Environ.* **231**, 111236 (2019).
167. Brown, J., Ferrians, Jr., O. J., Heginbottom, J. A. & Melnikov, E. S. *Circum-Arctic Map of Permafrost and Ground Ice Conditions* (National Snow and Ice Data Center, 2001).
168. Luthin, J. N. & Guymon, G. L. Soil moisture-vegetation-temperature relationships in central Alaska. *J. Hydrol.* **23**, 233–246 (1974).
169. Lachenbruch, A. H. Thermal effects of the ocean on permafrost. *Geol. Soc. Am. Bull.* **68**, 1515 (1957).
170. Hoelzle, M. & Gruber, S. in *Proc. Ninth Int. Conf. Permafrost* Vol. 2 (eds Kane, D. L. & Hinkel, K. M.) 723–728 (Inst. Northern Engineering, Univ. Alaska, 2008).
171. Smith, M. W. & Riseborough, D. W. Climate and the limits of permafrost: a zonal analysis. *Permafr. Periglac. Process.* **13**, 1–15 (2002).
172. Lachenbruch, A. H. & Marshall, B. V. Changing climate: geothermal evidence from permafrost in the Alaskan Arctic. *Science* **234**, 689–696 (1986).
173. Cuesta-Valero, F. J., García-García, A., Beltrami, H., González-Rouco, J. F. & García-Bustamante, E. Long-term global ground heat flux and continental heat storage from geothermal data. *Clim. Past.* **17**, 451–468 (2021).
174. Isaksen, K., Mühll, D. V., Gubler, H., Kohl, T. & Sollid, J. L. Ground surface-temperature reconstruction based on data from a deep borehole in permafrost at Janssonhaugen, Svalbard. *Ann. Glaciol.* **31**, 287–294 (2000).

Acknowledgements
The authors acknowledge support from the Geological Survey of Canada of Natural Resources Canada, the Norwegian Meteorological Institute, the WSL Institute for Snow and Avalanche Research SLF, MeteoSwiss and the Federal Office for the Environment and the Swiss Academy of Sciences, and the University of Alaska Fairbanks. S. Wolfe (Geological Survey of Canada) provided helpful comments on the manuscript.

Author contributions
S.L.S. and H.B.O'N. conceived and drafted the paper. All authors contributed to the provision of information, editing and revisions.

Competing interests
The authors declare no competing interests.

Peer review information
Nature Reviews Earth & Environment thanks Hanne Christiansen, Lin Zhao and the other, anonymous, reviewer(s) for their contribution to the peer review of this work.

Publisher's note
Springer Nature remains neutral with regard to jurisdictional claims in published maps and institutional affiliations.

Supplementary information
The online version contains supplementary material available at https://doi.org/10.1038/s43017-021-00240-1.

RELATED LINKS
CALM network: https://www2.gwu.edu/~calm
Global Climate Observing System: https://gcos.wmo.int/en/home
Global Terrestrial Network for Permafrost: https://gtnp.arcticportal.org/